PHYSICAL REVIEW B VOLUME 57, NUMBER 8 15 FEBRUARY 1998-II

Reconstructed pseudomorphic Co films on the Cr(110) surface

S. Fölsch, A. Helms, A. Steidinger, and K. H. Rieder
Institut für Experimentalphysik, Freie Universität Berlin, Arnimallee 14, D-14195 Berlin, Germany
(Received 9 September 1997)

Ultrathin epitaxial Co films on Cr(110) are examined by high-resolution low-energy electron diffraction. Pseudomorphic Co growth occurs over the entire coverage range investigated, i.e., up to 30 ML. A periodic lattice distortion is observed to exist in two equivalent (3×1) reconstruction domains showing uniaxial superperiodicity along either one of the two in-plane close-packed row directions. The lattice reconstruction is extended over several atomic layers normal to the surface. It is concluded that the overlayer reconstructs due to the constraint to adopt an inherently unstable structure forced by pseudomorphism. [S0163-1829(98)50108-7]

Metallic superlattices represent a class of modulated materials that show exceptional electronic and magnetic properties.[1] A prominent example of fundamental as well as technological relevance is the giant magnetoresistance (GMR) effect,[2] which is closely related to antiferromagnetic interlayer exchange coupling discovered in Fe/Cr superlattices[3] and later extensively studied for various other metal combinations.[4] Apart from strong interlayer exchange coupling, Co/Cr multilayers are of special interest because of their potential applicability to perpendicular magnetic recording.[5] For this particular metal combination, however, mutual epitaxy is complicated by the mismatched equilibrium crystal structures of Co (hcp) and Cr (bcc). The attempt to stabilize pseudomorphic Co with body-centered-cubic symmetry [which is obtained as a forced structure on GaAs(110) (Ref. 6)] within crystalline Co/Cr superlattices has not succeeded so far. On Cr(100), pseudomorphic Co growth occurs for the first few monolayers followed by continuous relaxation towards hcp structure.[7] Furthermore, textured[5,8] and semiepitaxial[9] Co/Cr(110) superlattices have been fabricated using various substrates. The existence of bcc Co in these systems still remains controversial.[5,8,9] In fact, recent theoretical work[10] has shown that bcc Co is unstable, while it exists in body-centered-tetragonal (bct) structure as a metastable phase. To illuminate the question of whether Co can be grown on Cr to pseudomorphic films of appreciable thickness we performed molecular-beam-epitaxy experiments using a Cr(110) substrate surface. It turns out that indeed pseudomorphic growth takes place over the entire coverage range investigated, that is, up to 30 ML. As a further remarkable feature, a (3×1) reconstruction is observed that is due to a periodic lattice distortion along in-plane close-packed atom row directions.

The investigations were performed under UHV conditions. Similar to preparation procedures given in literature,[11] a chemomechanical polished Cr(110) crystal was cleaned by simultaneous Ne^+ sputtering (800 eV, $I_0\sim3\,\mu$A) and annealing at 900 K. After repeated preparation cycles no residual nitrogen (the main bulk contamination[11]) was detectable by x-ray photoelectron spectroscopy (XPS). A (1×1) low-energy electron diffraction (LEED) pattern showing bright and sharp spots proved that this cleaning procedure leads to a smooth and well-ordered Cr(110) surface with a defect-free length of ~500 Å. Co was deposited from an electron-beam evaporator at a rate of ~0.5 Å/min. Films grown were investigated by *high-resolution LEED*, which provides information on structural features and surface roughness.[12] The latter can be directly probed during growth by *in situ* measurement of the specular beam intensity for out-of-phase scattering,[13] (i.e., destructive interference between electron waves scattered at adjacent terraces of the rough surface). In the present case, damped oscillations occur for growth temperatures between 270 and 400 K, indicating imperfect layer-by-layer growth.[13] At a growth temperature of 500 K, which is in the range of optimized temperatures for Co/Cr superlattice fabrication,[7] the oscillations give way to constant specular beam intensity that remains unchanged with proceeding coverage. This indicates that adatoms essentially nucleate at residual surface steps (step-flow growth[13]), i.e., the film retains a smooth growth front. Consistently, no spot broadening[13] is observed for out-of-phase scattering in this temperature regime, while it occurs for lower growth temperatures. For the investigations discussed in the following, the growth temperature was adjusted to 500 K.

A complementary check of film uniformity is achieved by analyzing the coverage-dependent evolution of XP intensities I_S and I_A specific for the substrate and the film, respectively. A corresponding data set of the Cr $2p$ and the Co $2p$ emission is shown in Fig. 1. The coverage is calibrated with the help of the growth oscillations observed in the low-temperature regime. In the upper panel the quantity $\ln[I_S/I_{S0}]$ is plotted vs coverage. The linear decay reveals that the measured substrate intensity I_S is well described by attenuation due to a film of uniform thickness d according to the simple relation $I_S=I_{S0}e^{-d/\lambda}$ with I_{S0} the emission intensity of the clean substrate and λ the mean free path of photoelectrons. Similarly, the linear coverage dependence of the quantity $\ln[1-I_A/I_{A0}]$ (lower panel) indicates that the measured Co $2p$ intensity follows the relation $I_A=I_{A0}[1-e^{-d/\lambda}]$ with the asymptotic intensity I_{A0} extracted from the atomic sensitivity factor ratio $S_{\mathrm{Co}\,2p}/S_{\mathrm{Cr}\,2p}$ that amounts to a value of 2.65 (Ref. 14). The λ value estimated from the data in Fig. 1 corresponds to the thickness of ~5 ML (equivalent to ~10 Å, cf. Fig. 5), in good agreement with the generally

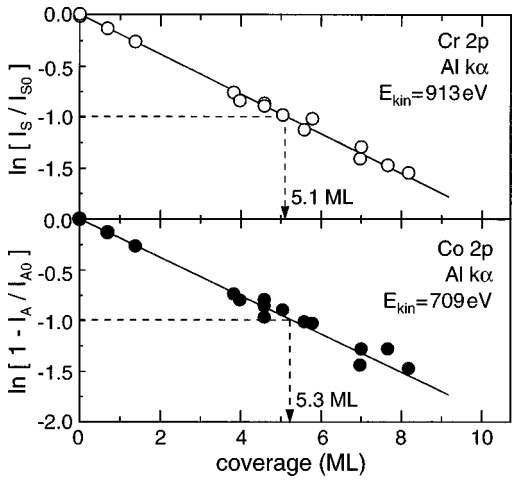

FIG. 1. Quantities $\ln[I_S/I_{S0}]$ and $\ln[1-I_A/I_{A0}]$ vs coverage with I_S and I_A as the coverage-dependent integral Cr $2p$ and Co $2p$ XP emission intensities.

observed mean free path of electrons as a function of kinetic energy.[15] It is thus excluded that significant intermixing or alloying takes place at the employed growth temperature of 500 K.

The structural analysis indicates the formation of pseudomorphic Co with a (3×1) lattice reconstruction. Figure 2(a) shows a related LEED pattern taken for a 5-ML-thick film. Equivalent diffraction patterns are observed over the entire temperature and coverage range investigated, i.e., up to 30-ML coverage and for growth temperatures between 220 and 500 K. As deduced from the positions of integral-order spots (denoted by integer indices) the crystallographic orientation of the overgrowth is in accordance with that of the Cr(110) substrate. Before discussing the coverage-dependent

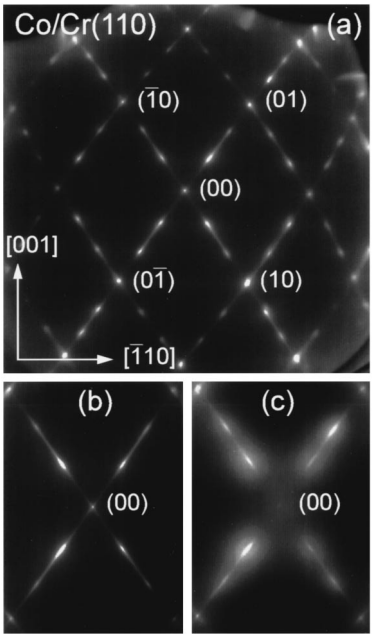

FIG. 2. LEED pattern of a 5-ML-thick Co/Cr(110) film at 125 eV showing (3×1) reconstruction (a). Lower panels show detailed scans at 133 eV for an 8-ML-thick film prior to (b) and after (c) removal of ~2 ML net coverage by Ne^+ sputtering.

evolution of the lattice parameters that confirms pseudomorphism, we address the present superstructure. It is composed of two equivalent (3×1) reconstruction domains, each of which implies an additional periodic correlation along respective close-packed row directions. The characteristic length of the superperiodicity is three times the nearest-neighbor spacing within a row. Third-order spots show pronounced broadening along the direction of superperiodicity while integral-order spots remain essentially sharp. Hence, the reconstruction is characterized by antiphase disorder,[16] i.e., the size of reconstruction domains is limited along the direction of threefold superperiodicity. Furthermore, the reconstruction proves to be robust in nature since it is not eliminated upon moderate sputtering: exposure of an 8-ML-thick Co film to Ne^+ bombardment at 100 K (500 eV, $I_0\sim1\,\mu$A, 15-min duration) removes a net coverage of ~2 ML (as revealed by XPS) and roughens the film surface. The latter is apparent from considerable spot broadening [cf. Figs. 2(b) and 2(c)] that shows up for scattering conditions deviating from in-phase scattering. It seems obvious that several layers are involved in the present reconstruction since the superstructure spots are not annihilated by the applied sputtering treatment. This suggestion is corroborated by the observed energy-dependent intensity variation of superstructure spots. It can be attributed in a straightforward way to the existence of additional Bragg reflections due to the presence of a (3×1) lattice reconstruction that is extended normal to the film surface.

To show this, it is instructive to visualize the reciprocal lattice of a bcc lattice that exhibits a superimposed threefold periodicity along either one of the two close-packed row directions within the (110) plane (i.e., the [111] or the [111] direction). If, for example, the [111] direction is chosen, the base that spans a corresponding primitive unit cell in real space is given by the triplet $\mathbf{a}=(3a_0/2)(-\mathbf{e}_x,\mathbf{e}_y,\mathbf{e}_z)$, $\mathbf{b}=(a_0/2)(\mathbf{e}_x,-\mathbf{e}_y,\mathbf{e}_z)$, and $\mathbf{c}=(a_0/2)(\mathbf{e}_x,\mathbf{e}_y,-\mathbf{e}_z)$, with a_0 denoting the cubic lattice constant and the translation $\mathbf{a}$ representing the uniaxial superperiodicity. Equivalently, a twin cell may be generated by combining the same in-plane translations $\mathbf{a}'=\mathbf{a}$ and $\mathbf{b}'=\mathbf{b}$, and the out-of-plane translation $\mathbf{c}'=(a_0/2)(\mathbf{e}_x,\mathbf{e}_y,\mathbf{e}_z)$. Transformation to the reciprocal base yields the triplet $\mathbf{a}^*=(2\pi/3a_0)(0,\mathbf{e}_y,\mathbf{e}_z)$, $\mathbf{b}^*=(2\pi/a_0)(\mathbf{e}_x,0,\mathbf{e}_z)$, and $\mathbf{c}^*=(2\pi/a_0)(\mathbf{e}_x,\mathbf{e}_y,0)$, or alternatively, $\mathbf{a}'^*=(2\pi/3a_0)(-\mathbf{e}_x,0,\mathbf{e}_z)$, $\mathbf{b}'^*=(2\pi/a_0)(0,-\mathbf{e}_y,\mathbf{e}_z)$, and $\mathbf{c}'^*=(2\pi/a_0)(\mathbf{e}_x,\mathbf{e}_y,0)$ for the twin. Hence, additional Bragg points that originate from the superperiodicity along [111] are located on the (111) plane, since $(\mathbf{a}^*\times\mathbf{a}'^*)\|[111]$. Figure 3 shows this projection of the reciprocal lattice with full lines as the (01), (00), and (01) reciprocal lattice rods, and dashed lines as third-order lattice rods of the (110) surface. Apart from determining surface periodicities, LEED also provides access to the crystal structure normal to the surface because primary electrons have finite penetration depth into the bulk.[15] The situation becomes especially transparent if the diffraction process is sufficiently well approximated by kinematic (i.e., single) electron scattering. In this case, energy-dependent intensity curves of diffraction beams are dominated by primary Bragg peaks.[17] Figure 4 shows the intensity of integral- and third-order spots along the [112] azimuth for a 5-ML-thick Co film. These intensity curves are compared with energy values expected

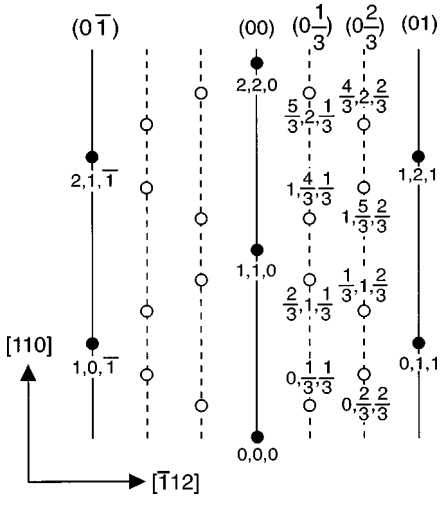

FIG. 3. Reciprocal lattice of a bcc crystal with superimposed threefold periodicity along [111]; the lattice is projected along the [111] direction. Full circles denote principal Bragg points located on integral-order lattice rods (full lines) while empty circles are third-order Bragg points due to the superperiodicity.

for kinematic scattering involving the Bragg points in Fig. 3. They were calculated for a cubic lattice constant of $a_0 = 2.88$ Å equal to that of the Cr host (i.e., perfect pseudomorphism was assumed). Indices on the right-hand side assign particular Bragg reflections to related energies. By inspecting at first the (00) and the (01) spots it is noted that major intensity maxima are located close to the energetic positions of integral-order Bragg points, thus corroborating that (i) the magnitude of diffracted intensity is predominantly determined by kinematic scattering and (ii) the overlayer indeed adopts a pseudomorphic structure. It is remarkable that systematic coincidence between measured intensity maxima and kinematic energy values is also fulfilled for the energy-dependent intensity variation of the third-order spots: pairs of solid and dashed lines in Fig. 4 mark energetic positions due to the additional third-order Bragg points expected for a superimposed threefold periodicity along [111] as discussed in connection with Fig. 3. This suggests that the presently observed third-order superstructure spots originate from a superimposed coherent lattice reconstruction, which involves several atomic layers of the pseudomorphic Co overlayer. Intensity curves equivalent to those in Fig. 4 are observed along the [112] azimuth, which confirms the existence of two equivalent reconstruction domains. It is likely that pseudomorphic strain is responsible for the presently observed (3×1) lattice reconstruction. Periodic lattice distortions are known to occur for forced structures that are imposed by pseudomorphism. A prominent example is the widely investigated system Fe/Cu(100):[18,19] for coverages <5 ML the Cu host stabilizes heavily reconstructed fcc Fe, which proves to be a precursor to the intrinsic bcc phase of iron finally formed in a martensitic phase transformation. The characteristic lattice reconstruction of the fcc-like precursor is due to the buckling of in-plane oriented close-packed atom rows.[19] It seems suggestive that a similar scenario also applies to the lattice reconstruction observed here, i.e., the overlayer reconstructs due to the constraint to adopt pseudomorphic structure.

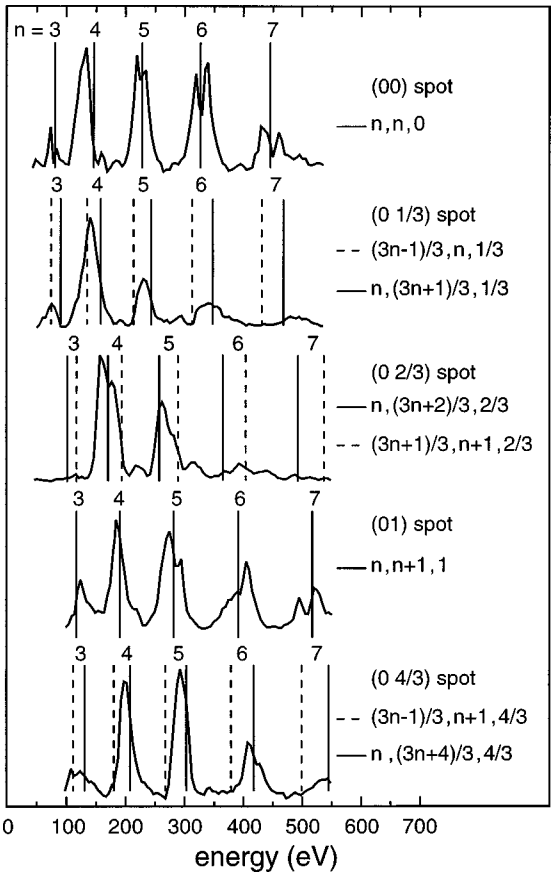

FIG. 4. Intensity of integral- and third-order spots along the [112] azimuth for 5-ML Co on Cr(110), indices on the right-hand side assign particular Bragg reflections to related energy values calculated for kinematic scattering.

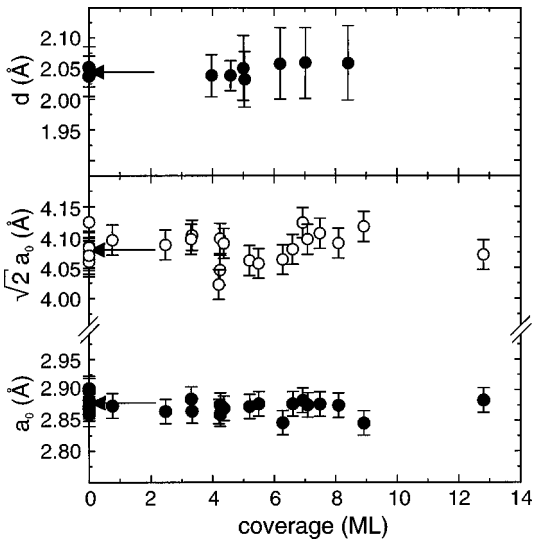

FIG. 5. Coverage-dependent evolution of interlayer spacing (upper panel) and lateral lattice parameters (lower panel); arrows denote lattice parameters expected for bulk Cr.

Finally, the coverage-dependent evolution of lateral and vertical lattice parameters is addressed. The upper panel of Fig. 5 shows the interlayer spacing estimated by fitting the energetic positions of primary Bragg peaks of the (00) spot according to the Laue condition that accounts for layer peri-

odicity normal to the surface.[17] In the lower panel, the lateral lattice parameters $\sqrt{2}a_0$ measured along [110] (empty circles) and a_0 measured along [001] (full circles) are plotted. They are extracted from integral-order spot positions in the diffraction pattern. Arrows denote respective lattice parameters of bulk Cr. Within the range of accuracy the lattice parameters essentially retain the values imposed by the substrate. It is thus unambiguously concluded that the overlayer is strained to pseudomorphic structure, i.e., the arrangement of Co atoms is characterized by body-centered-cubic symmetry [aside from superimposed displacements leading to (3×1) reconstruction]. On the other hand, there is no clear evidence for the actual equilibrium crystal phase, i.e., the crystal phase from which the overlayer is strained to pseudomorphic structure. A quantitative strain analysis to verify the compatibility of measured strains with potential equilibrium structures is not justified on the basis of our data, because the reliability of the estimated interlayer spacing obtained here is not comparable with that of *quantitative LEED* (QLEED) analysis.[17,18] Future QLEED investigations for precise structure analysis are thus desirable. In principle, Co may exist in three different crystal phases:[10,18] stable hcp structure ($a=2.51$ Å, $c/a=1.62$), metastable fcc structure ($a=3.54$ Å), and metastable bct structure ($a=2.91$ Å, $c/a=0.92$). Each of these provide particular lattice planes that, if sufficiently strained, are likely candidates to match the Cr(110) plane. For a bct structure these are a (110) plane or a (011) plane (which are nonequivalent due to the tetragonal distortion along [001]), a (111) plane for fcc structure, and a (0001) plane for hcp structure. Related lattice misfit considerations may provide a guideline for quantitative strain analysis; nonetheless, they have to be taken with caution since the present situation is further complicated by the existence of a lattice reconstruction.

In conclusion, the presently observed stabilization of smooth pseudomorphic Co films several tens of angstroms in thickness meets an essential precondition for potential future fabrication of crystalline Co/Cr(110) superlattices. As a remarkable detail, a periodic lattice distortion occurs that exists in two equivalent reconstruction domains with threefold uniaxial superperiodicity along either one of the two in-plane close-packed row directions. We propose that the driving force of this lattice reconstruction is pseudomorphic strain. Beyond the determination of periodic correlations as presented here, it is desirable (i) to uncover the atomic structure of the (3×1) lattice reconstruction and (ii) to clarify the actual equilibrium crystal phase of the pseudomorphically strained overlayer. For this task we encourage future QLEED investigations. Furthermore, it would be interesting to probe the magnetic properties of this structural modification of Co.

Support by the Deutsche Forschungsgemeinschaft, Sfb 290, is gratefully acknowledged.

[1] C. M. Falco and I. K. Schuller, in *Synthetic Modulated Structures*, edited by L. L. Chang and B. C. Giessen (Academic, Orlando, 1985).
[2] M. N. Baibich *et al.*, Phys. Rev. Lett. **61**, 2472 (1988).
[3] P. Grünberg, R. Schreiber, Y. Pang, M. B. Brodsky, and C. H. Sowers, Phys. Rev. Lett. **57**, 2442 (1986).
[4] S. S. P. Parkin, Phys. Rev. Lett. **67**, 3598 (1991).
[5] N. Sato, J. Appl. Phys. **61**, 1979 (1987).
[6] G. A. Prinz, Phys. Rev. Lett. **54**, 1051 (1985).
[7] N. Metoki, W. Donner, and H. Zabel, Phys. Rev. B **49**, 17 351 (1994).
[8] M. B. Stearns, C. H. Lee, and T. L. Groy, Phys. Rev. B **40**, 8256 (1989); P. Boher, F. Giron, P. Houdy, P. Beauvillain, C. Chappert, and P. Veillet, J. Appl. Phys. **70**, 5507 (1991).
[9] Y. Herny, C. Mény, A. Dinia, and P. Panissod, Phys. Rev. B **47**, 15 037 (1993).
[10] A. Y. Liu and D. J. Singh, Phys. Rev. B **47**, 8515 (1993); P. Alippi, P. M. Marcus, and M. Scheffler, Phys. Rev. Lett. **78**, 3892 (1997).
[11] N. D. Shinn and T. E. Madey, J. Chem. Phys. **83**, 5928 (1985).
[12] J. Wollschläger, J. Falta, and M. Henzler, Appl. Phys. A: Solids Surf. **50**, 57 (1990).
[13] M. Henzler, Prog. Surf. Sci. **42**, 297 (1993).
[14] *Handbook of X-Ray Photoelectron Spectroscopy*, edited by G. E. Muilenberg (Perkin-Elmer Corp., Eden Prairie, 1979).
[15] M. P. Seah and W. A. Dench, Surf. Interface Anal. **1**, 2 (1979).
[16] M. Henzler, in *Electron Spectroscopy for Surface Analysis*, edited by H. Ibach (Springer, New York, 1977).
[17] M. A. Van Howe, W. H. Weinberg, and C.-M. Chan, in *Low-Energy Electron Diffraction*, Vol. 6 of *Springer Series in Surface Science*, edited by G. Ertl (Springer, New York, 1986).
[18] F. Jona and P. M. Marcus, Crit. Rev. Surf. Chem. **4**, 189 (1994).
[19] S. Müller, P. Bayer, C. Reischl, K. Heinz, B. Feldmann, H. Zillgen, and M. Wuttig, Phys. Rev. Lett. **74**, 765 (1995).